Effect of Trisodium Citrate on the Morphology and Luminescence Properties of Hydrothermally Synthesized YVO_4 Phosphor

Sa Zhang[a], Yan Liang[b] and Xiaoyong Gao[a,*]

[a]School of Physics and Engineering, Zhengzhou University, Zhengzhou 450052, China

[b]College of Information Science and Engineering, Henan University of Technology, Zhengzhou 450001, China

(Received March 12, 2015; in final form December 24, 2015)

YVO_4 phosphors with different morphologies were synthesized by trisodium citrate (Na_3cit) surfactant-assisted hydrothermal process. Effects of molar ratio of cit^{3-} to Y^{3+} and pH value of reaction solution were intensively investigated on the morphologies, structures and luminescence properties of YVO_4 phosphor. The morphologies of the YVO_4 particles can be effectively controlled in strong acidic and strong alkaline environment by affecting the adsorption of cit^{3-} on the (001) crystal plane of YVO_4. Strong acidic condition resulted into excessive adsorption of cit^{3-} groups on the YVO_4 phosphor, which annihilated the superior luminescence of YVO_4 phosphors. On the contrary, strong alkaline condition does not result into the adsorption of cit^{3-} groups. The synthesized YVO_4 phosphor without adsorption of cit^{3-} groups showed superior luminescence even though the effective control of the morphology in alkaline condition is not so good as in strong acidic condition.

DOI: 10.12693/APhysPolA.129.79

PACS: 78.55.–m, 61.05.cp, 68.37.Hk, 78.30.–j

1. Introduction

In recent years, inorganic nano/micromaterials have been widely used in photoelectrics, medicine, catalysis, and other fields due to the particularity of their size and structure. The synthesis of inorganic nano/microcrystals with well-defined morphologies and accurate tunable sizes remains a focus of research and a challenging issue considering that the properties of these materials are closely interrelated with geometric factors, such as shape, dimensionality, and size [1]. Yttrium vanadate (YVO_4) is widely used in the fields of luminescence [2], catalysts [3], and laser host materials [4] because of its excellent thermal stability, mechanical properties, and optical properties. However, for the preparation of YVO_4 nano/microcrystals, especially nano/microparticles, the small size effect (i.e. large surface area and high surface energy) facilitates agglomeration [1]. When not dispersed, their excellent performance may be affected. Therefore, the particular shape and size of the synthesized YVO_4 nano/microparticles have a certain practical significance in optimizing their properties. The hydrothermal method is widely used because it is conducive for the full complexation and reaction between surfactants and reactants to effectively control the product morphology. The surface physical modification of YVO_4 nano/microparticles can be realized by adding suitable surfactants in the reaction solution [5]; subsequently, monodisperse YVO_4 nano/microparticles with various morphologies can be obtained. Qian et al. synthesized nano/micro YVO_4 phosphors with morphologies of nanoparticle, persimmon spherical, and cube-shaped multi-level assembly structures using sodium citrate, sodium tartrate, and sodium malate as surfactants, respectively [6]. Xu et al. synthesized nano/micro YVO_4 phosphors with morphologies of persimmon spherical, cubic block, cubic columnar, and grain-like self-assembled structures using sodium citrate, ammonium oxalate, ethylenediamine tetraacetic acid disodium salt, and polyvinylpyrrolidone as surfactants, respectively [7]. They studied the formation mechanism of the persimmon spherical structure. Authors themselves once fabricated YVO_4 phosphor powders by using hydrothermal method. They carefully studied the effect of hydrothermal temperature on the microstructure, the absorption and luminescent properties of the phorphor powders [8]. Besides, they also fabricated spherical YVO_4 phosphor powders at molar ratio of cit^{3-} to Y^{3+} of 2:1 by using hydrothermal method and studied the effect of the annealing temperature on the microstructure and the luminescent properties [9]. However, systematic research of pH values of reaction solution is rarely available on the effective control of morphology of YVO_4 phosphors in the hydrothermal process. Therefore, in this paper, YVO_4 nano/microparticles with specific size and morphology were synthesized using trisodium citrate (Na_3cit) as surfactant and different pH values. Effects of molar ratio of cit^{3-} to Y^{3+} (cit^{3-}:Y^{3+}) and pH value of reaction solution were intensively investigated on the morphologies, structures and luminescence properties of YVO_4 phosphor. Further analysis of the effect of pH value was also done on effective control of the morphology of YVO_4 phosphors assisted by a Na_3cit surfactant.

*corresponding author; e-mail: xygao@zzu.edu.cn

2. Experimental

2.1. Synthesis of the YVO_4 phosphor

A suitable amount of Y_2O_3 (purity: 99.99%) was dissolved in hydrochloric acid at an elevated temperature to prepare a 0.2 M YCl_3 solution. Specific amounts (0, 0.004, 0.008, 0.012, 0.016, 0.008, and 0.008 mol) of Na_3cit were respectively added into backers containing 40 mL deionized water. The backers were numbered 1 to 7 in sequence. After the Na_3cit was dissolved, 20 mL of 0.2 M YCl_3 was added into each backer. Following vigorous stirring for 1 h, 0.004 mol of Na_3VO_4 (99.9%) was introduced into each of the seven backers. Then, the pH values of the solutions in backers 1 to 5 were adjusted to 3 and the pH value in backer 6 to 7 by using hydrochloric acid. Additionally, the pH value in backer 7 was adjusted to 10 by using NaOH solution. After additional agitation for 1 h, the obtained mixed solution were transferred into teflon bottles held in a stainless steel autoclave, sealed, and maintained at 180 °C for 24 h. As the autoclave cooled to room temperature, the precipitates were separated by centrifugation, washed with ethanol and deionized water in sequence, and then air dried at 80 °C for 12 h. Subsequently, the YVO_4 phosphor powders were obtained.

2.2. Characterization

The crystallization, vibration modes, and surface morphology of the YVO_4 phosphor powders were determined through X-ray diffraction (XRD, Philips PANAlytical X'pert), Raman spectroscopy (Renishaw 2000), and cold field emission scanning electron microscopy (CF-SEM, JEOL-JSM-6700F), respectively. The luminescent properties were measured through a spectrofluorometer (FluoroMax-4). All measurements were carried out at room temperature.

3. Results and discussion

3.1. Surface morphology and formation mechanism

Figure 1 shows the SEM images of the YVO_4 phosphors synthesized at different cit^{3-}:Y^{3+} molar ratios and pH values. In the acidic solution of pH = 3, the YVO_4 phosphor samples synthesized with different cit^{3-}:Y^{3+} (0:1, 1:1, 2:1, 3:1, and 4:1), respectively, have a regular octahedron with irregular flake self-assembled structures, some spherical particles and some lamellar structures, uniform mono-disperse spherical particles, some spherical particles and some pillar structures assembled by some spherical particles along a fixed direction, and some scattered lamellar particles and a large number of pillar structures assembled by spherical particles. In the neutral solution of pH = 7, the YVO_4 phosphor synthesized using a cit^{3-}:Y^{3+} of 2:1 has uniform spherical nanoparticle morphology. By contrast, in the alkaline solution of pH = 10, the YVO_4 phosphor synthesized with cit^{3-}:Y^{3+} of 2:1 has irregular microparticle morphology. Therefore, in addition to the internal structure of the YVO_4 crystal itself, the formation of different surface morphologies of the YVO_4 phosphors is also possibly determined by the control of YVO_4 crystal growth process as influenced by the pH and the cit^{3-}:Y^{3+}. Vanadate, which is sensitive to the pH of a solution, exists in the form of $V_{10}O_{28}^{6-}$ at pH = 3, whereas it exists in the form of VO_4^{3-} at pH = 10 [10]. Li et al. synthesized YVO_4 nanobelts without any surfactant at pH = 1 [11]. This result is attributed to the high H^+ concentration in strong acidic solution. At pH = 1, H^+ cannot perturb YVO_4 growth along the [010] direction, and the rate is faster than in other directions. The faster rate limits the anisotropic growth of YVO_4 and leads to the formation of belt-like YVO_4 nanostructures [11]. When the pH increases to 3, considering the preferential ionic interaction, OH^- competes with $V_{10}O_{28}^{6-}$ during the hydrothermal process and avoids [010] direction growth. Hence, anisotropic growth is not perturbed, and the final morphologies of the YVO_4 are octahedral and irregular flake self-assembled structures [11].

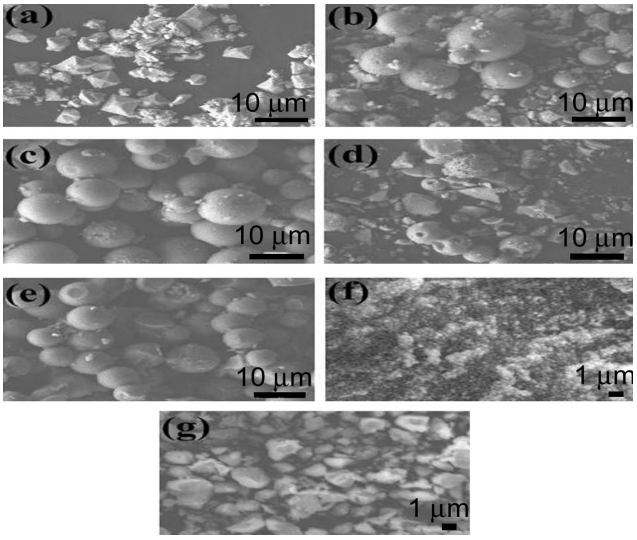

Fig. 1. SEM images of the YVO_4 phosphors synthesized at (a) pH = 3, cit^{3-}:Y^{3+} = 0:1, (b) pH = 3, cit^{3-}:Y^{3+} = 1:1, (c) pH = 3, cit^{3-}:Y^{3+} = 2:1, (d) pH = 3, cit^{3-}:Y^{3+} = 3:1, (e) pH = 3, cit^{3-}:Y^{3+} = 4:1, (f) pH = 7, cit^{3-}:Y^{3+} = 2:1, (g) pH = 10, cit^{3-}:Y^{3+} = 2:1.

Initially, cit^{3-}, a strong chelating agent with three carboxylate groups for metal ions, reacts with Y^{3+} to form stable $[Y(cit)_2]$ complexes through a stronger coordination interaction in the acidic solution when Na_3cit is added as surfactant [12]. Then, under hydrothermal conditions (high temperature and pressure), the $[Y(cit)_2]$ complexes are attacked by $V_{10}O_{28}^{6-}$, and cit^{3-} is gradually replaced by $V_{10}O_{28}^{6-}$. YVO_4 crystal nuclei are formed after the $V_{10}O_{28}^{6-}$ depolymerizes to VO_4^{3-}. This competition reaction can slow down the nucleation and subsequent crystal growth of YVO_4 nuclei. During the subsequent crystal growth stage, cit^{3-} separated from $[Y(cit)_2]$

complexes are adsorbed selectively on the active (001) facet of the YVO_4 nuclei. Thus, crystal growth along the [001] orientation, to some extent, is inhibited, and it grows preferentially along the [100] and [010] directions. Hence, primary nanosheet structural YVO_4 is formed. Given that the top and bottom of these primary nanostructural YVO_4 are (001) planes, the surface energy of YVO_4 nanosheets are reduced by accumulating along the [001] direction in the presence of static electrical force caused by cit^{3-}. Then, these assemble into a spherical structure and grow through the Ostwald process [6].

Our results show that complexes of low coordination number are formed by cit^{3-} and Y^{3+} when the cit^{3-}:Y^{3-} is 1:1. Moreover, Y^{3+} ions are released quickly, which accelerate the nucleation rate of the YVO_4 nuclei and the formation of partial spherical particles and partial unformed YVO_4 sheet-like structures. Increasing the cit^{3-}:Y^{3+} to 2:1 facilitates the formation of $[Y(cit)_2]$ complexes, which slows down the release rate of Y^{3+} and finally forms the monodisperse YVO_4 microparticles with spherical structure. Upon further increase the amount of cit^{3-}, the cit^{3-}:Y^{3+} is increased to 3:1. The morphologies of the sample include some spherical YVO_4 particles and some columnar structures assembled by spherical particles through the strong electrostatic interactions of cit^{3-} along the [001] direction. At the higher ratio of 4:1, more columnar self-assembled structures are formed. In general, the morphology of the sample synthesized in acidic solution at pH = 3 is spherical microparticles, which may be attributed to the adsorption of the higher concentration of H^+ on the surface of YVO_4 particles. During the crystal growth stage, given the strong interaction between negative and positive charges, cit^{3-} can easily be adsorbed on the (001) plane of YVO_4 nuclei, which is more conducive to the control of the morphology of YVO_4 particles. By contrast, in the neutral solution of pH = 7 the products synthesized with cit^{3-}:Y^{3+} of 2:1 has nanoparticle morphology. This result may be attributed to the decrease in H^+ concentration as the pH value of the reaction solution increases. The reduced interaction between positive and negative ions is non-conducive for the effective adsorption of the cit^{3-} group on the (001) plane of YVO_4 particles and the self-assembly process caused by the static electrical force among the cit^{3-} groups. In the solution with pH = 10 and cit^{3-}:Y^{3+} = 2:1, the control of YVO_4 particle morphology is not evident, and the particles aggregate to a great extent.

3.2. Crystallization and vibration modes

Figure 2 shows the XRD patterns of the YVO_4 phosphors synthesized using the hydrothermal method at different cit^{3-}:Y^{3+} and pH values. JCPDS 17-0341 is the standard diffraction pattern of a tetragonal YVO_4 crystal. Figure 2a shows that the product synthesized with cit^{3-}:Y^{3+} = 0:1 and pH = 3 exhibits the tetragonal and polycrystalline structure of the YVO_4 phase. Figure 2b shows that the product synthesized with cit^{3-}:Y^{3+} = 2:1 and pH = 3 does not show the YVO_4 characteristic diffraction peaks, which may be attributed to the adsorption of a large number of amorphous cit^{3-} groups on the surface of the YVO_4 particles. The cit^{3-} groups can shield the XRD information of YVO_4. The XRD patterns of products synthesized using cit^{3-}:Y^{3+} = 1:1, 3:1, 4:1 and pH = 3 are similar to Fig. 2b, which indicates that the surface of the products can easily adsorb the cit^{3-} groups in acidic solution. By contrast, the products synthesized using cit^{3-}:Y^{3+} = 2:1 and pH = 7, 10 are tetragonal polycrystalline YVO_4 particles, which is different from the products synthesized at pH = 3. Therefore, the adsorption of cit^{3-} on the surface of YVO_4 particles is not apparent in the neutral and alkaline solution.

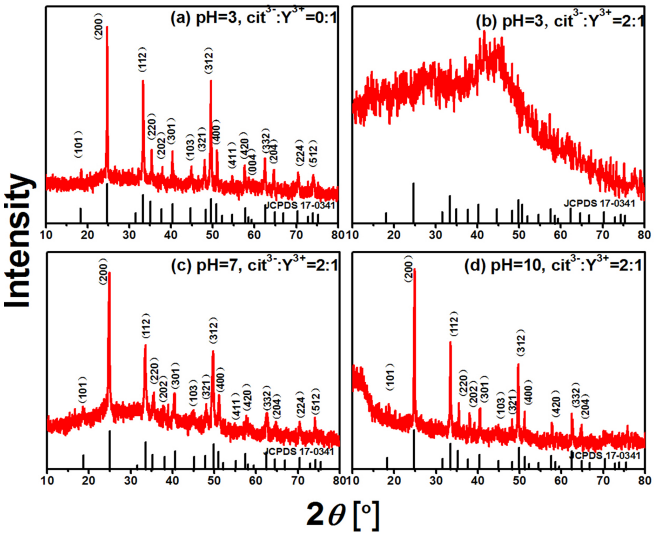

Fig. 2. X-ray diffraction patterns of the YVO_4 phosphors synthesized using the hydrothermal method at (a) pH = 3, cit^{3-}:Y^{3+} = 0:1, (b) pH = 3, cit^{3-}:Y^{3+} = 2:1, (c) pH = 7, cit^{3-}:Y^{3+} = 2:1; (d) pH = 10, cit^{3-}:Y^{3+} = 2:1.

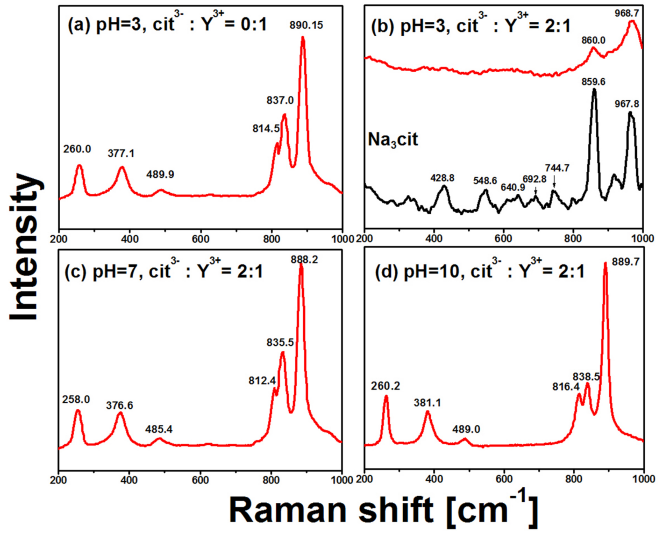

Fig. 3. Raman spectra of the YVO_4 phosphors synthesized at (a) pH = 3, cit^{3-}:Y^{3+} = 0:1, (b) pH = 3, cit^{3-}:Y^{3+} = 2:1, (c) pH = 7, cit^{3-}:Y^{3+} = 2:1, (d) pH = 10, cit^{3-}:Y^{3+} = 2:1.

To further confirm the results, we tested the YVO_4 phosphor powders using the Raman spectroscopy with an excitation wavelength of 532 nm. The vibration modes are shown in Fig. 3. The six Raman shift peaks of YVO_4 synthesized at pH = 3 and cit^{3-}:Y^{3+} = 0:1 (Fig. 3a) are located at 260.0, 377.1, 489.9, 814.5, 837.0, and 890.15 cm^{-1}, which originate from the internal vibrations of the vanadium–oxygen tetrahedron; the results are consistent with the literature [13]. Figures 3c and d are similar to Fig. 3a, which indicates that the YVO_4 particles synthesized at pH = 7 and 10 using cit^{3-}:Y^{3+} of 2:1 still exhibit tetragonal structure. However, the position of the peaks are slightly different compared with the corresponding peaks in Fig. 3a, which may be attributed to the differences in crystallization of YVO_4 particles with the presence of Na_3cit. Two obvious peaks located at 860.0 and 968.7 cm^{-1} were found in the Raman spectrum of the product synthesized at pH = 3 using cit^{3-}:Y^{3+} of 2:1, which do not correspond to the characteristic peaks of YVO_4. To understand the two new Raman peaks, we also tested the Raman spectrum of the Na_3cit powder. The peaks located at 859.6 and 967.8 cm^{-1} correspond to the vibration modes of the cit^{3-} group. Hence, we confirmed the presence of a large number of cit^{3-} groups adsorbed on the surface of YVO_4 particles in the acidic solution with pH = 3.

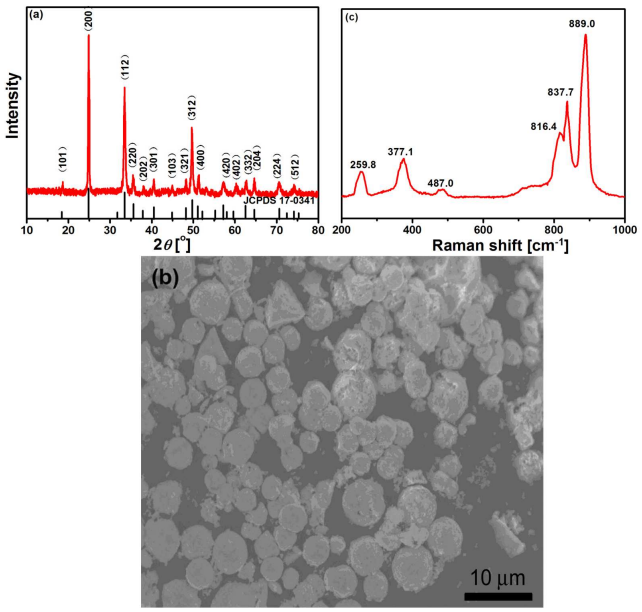

Fig. 4. Properties characterization for the sample synthesized using pH = 3 and cit^{3-}:Y^{3+} of 2:1 after annealed at 900 °C in the air for 1 h: (a) XRD pattern, (b) SEM image, (c) Raman spectrum.

To demonstrate the synthesis of YVO_4 at pH = 3 using cit^{3-}:Y^{3+} of 2:1, the sample was annealed at 900 °C in the air for 1 h (Fig. 4) to completely remove the cit^{3-} groups adsorbed on the surface of YVO_4 particles by physical means. After annealing at 900 °C for 1 h, the characteristic diffraction peaks and Raman shift peaks of YVO_4 in the XRD and Raman spectra confirmed the synthesis of YVO_4 at pH = 3 using cit^{3-}:Y^{3+} of 2:1. After annealing, the surface of the sample became rough and the size of the particles became smaller, which may be caused by the desorption of C and H elements in cit^{3-} groups in the form of CO_2 and H_2O vapor after reacting with O_2 in air.

3.3. Luminescent properties

The photoluminescent properties of YVO_4 phosphors (Fig. 5) were tested using a spectrophotometer. YVO_4 has a wide absorption band (200–320 nm) rather than a sharp absorption edge. Hence, the excitation wavelength was 300 nm determined in terms of the absorption spectrum reported elsewhere [8] rather than excitation spectrum. The range of the test wavelength was 340 nm to 800 nm. When excited by 300 nm ultraviolet photons, the luminescent centers of the YVO_4 phosphors synthesized at pH = 3 using cit^{3-}:Y^{3+} of 1:1, 2:1, 3:1, and 4:1 are located at 400 nm, consistent with the position of the luminescent peak of the Na_3cit powder and different from the characteristic emission of VO_4^{3-} ions in the visible region [14]. The emission peak around 400 nm is attributed to the characteristic emission of the cit^{3-} group adsorbed on the surface of the YVO_4 phosphors. The YVO_4 phosphors synthesized at pH = 3 using cit^{3-}:Y^{3+} of 0:1, and at pH = 7 and 10 using cit^{3-}:Y^{3+} of 2:1 show the characteristic emission band of VO_4^{3-} in the visible region, and so does the YVO_4 phosphors annealed at 900 °C for 1 h at pH = 3 using cit^{3-}:Y^{3+} of 2:1. Compared with the sample without Na_3cit surfactant, a blueshift of the emission center of VO_4^{3-} is, to a certain extent, observed in the emission spectra of the other unannealed samples.

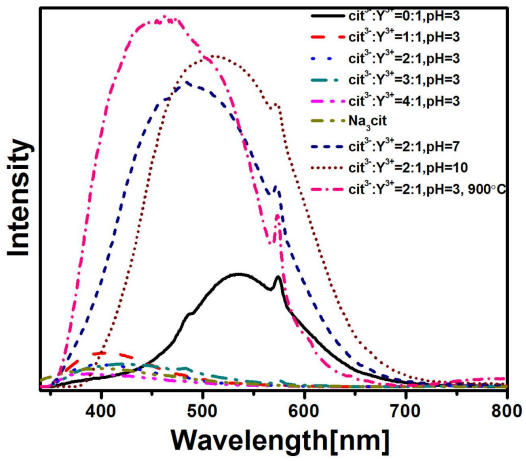

Fig. 5. Photoluminescence spectra of the YVO_4 phosphors synthesized under different conditions.

The blue shift may be attributed to the higher crystalline quality of YVO_4 phosphors promoted by the addition of cit^{3-} in the neutral and alkaline solutions. The energy of the V–O bond in VO_4^{3-} increases to a certain degree, which results in the emission of visible light with a different energy through various phonon relaxation processes

after excitation by ultraviolet photons. The annealed sample has the maximum luminous intensity, which may be attributed to the full desorption of cit^{3-} groups from the sample and the large increase in crystallinity of the YVO_4 phosphor. However, the photoluminescence emission spectra of all samples, except for Na_3cit, have weak peaks located at 481 and 573 nm, which may be due to a few Dy^{3+} ions present in the Y_2O_3 raw materials [15]. The emission intensity of the samples at pH = 3, 7, and 10 using cit^{3-}:Y^{3+} of 2:1 show that the amount of cit^{3-} groups effectively adsorbed on YVO_4 particles reduces gradually, as well as the control of morphologies of the samples; whereas, the luminous intensity of the samples increases gradually with the increase in pH value. This may be attributed to the –OH and –COOH functional groups exhibiting high vibration energies in the cit^{3-} groups adsorbed on YVO_4 particles, which may extinguish the light emission and effectively weaken the radiative transition probability of excited VO_4^{3-} ions from the excited state to the ground state.

4. Conclusions

In this study, nano/microparticles of YVO_4 phosphors with different morphologies were synthesized by Na_3cit surfactant-assisted hydrothermal process. Influences on the morphologies, structures, and optical properties of YVO_4 phosphors caused by different cit^{3-}:Y^{3+} and pH values were investigated. For YVO_4 phosphor with cit^{3-}:Y^{3+} of 2:1, the pH value greatly affects the morphologies of the samples. This process is accomplished through the adsorption effectiveness of cit^{3-} groups on the (001) plane of the YVO_4 crystal. As the pH increases, the effective control of the morphology of YVO_4 phosphor powder is gradually reduced, whereas the luminescence intensity gradually increases. Strong acidic condition contributes to the effective adsorption of cit^{3-} groups on the surface of the YVO_4 particles, annihilating the superior luminescence of YVO_4 phosphors. After annealing at 900 °C for 1 h in air, the cit^{3-} groups adsorbed on YVO_4 particles can be removed effectively and the characteristic emission of YVO_4 phosphor powder is exhibited. However, the synthesized YVO_4 phosphors in strong alkaline condition have no obvious adsorption of cit^{3-} groups and show superior luminescent properties even though the effective control of the morphologies is not so good as in strong acidic condition.

Acknowledgments

Authors are grateful for the supports by the National Natural Science Foundation of China (grant No. 60807001), the Foundation of Young Key Teachers from University of Henan Province (grant No. 2011GGJS-008), and the Foundation of Henan Educational Committee (grant No. 2010A140017).

References

[1] L.D. Zhang, J.M. Mou, *Nanomaterials and Nanostructures*, Science Press, Beijing 2001, p. 62 (in Chinese).

[2] Y. Terada, K. Shimamura, V.V. Kochurikhin, L.V. Barashov, M.A. Ivanov, T. Fukuda, *J. Cryst. Growth* **167**, 369 (1996).

[3] Z.M. Fang, Q. Hong, Z.H. Zhou, S.J. Dai, W.Z. Weng, H.L. Wan, *Catal. Lett.* **61**, 39 (1999).

[4] R.A. Fields, M. Bimbaum, C.L. Fincher, *Appl. Phys. Lett.* **51**, 1885 (1987).

[5] B.S. Xu, *Nano Surface Engineering*, Chemical Industry, Beijing 2004 (in Chinese).

[6] L.W. Qian, Ph.D. Thesis, Shanghai Jiao Tong University, Shanghai 2009 (in Chinese).

[7] Z.H. Xu, X.J. Kang, C.X. Li, Z.Y. Hou, C.M. Zhang, D.M. Yang, G.G. Li, J. Lin, *Inorg. Chem.* **49**, 6706 (2010).

[8] S. Zhang, Y. Liang, X.Y. Gao, H.T. Liu, *Acta Phys. Pol. A* **125**, 105 (2014).

[9] S. Zhang, Y. Liang, X.Y. Gao, H.T. Liu, *Chinese Journal of Vacuum Science and Technology* **34(7)**, 768 (2014) (in Chinese).

[10] K. Tang, M.L. Huang, J.Y. Yang, F.D. Yu, G.L. Shang, J.H. Wu, *J. Synth. Cryst.* **40**, 1429 (2011) (in Chinese).

[11] G.C. Li, K. Chao, H.R. Peng, K.Z. Chen, *J. Phys. Chem. C* **112**, 6228 (2008).

[12] A. Huignard, V. Buissette, G. Laurent, T. Gacoin, J.P. Boilot, *Chem. Mater.* **14**, 2264 (2002).

[13] B. M. Jin, S. Erdei, A.S. Bhalla, F.W. Ainger, *Mater. Res. Bull.* **30**, 1293 (1995).

[14] H. Ronde, G. Blasse, *J. Inorg. Nucl. Chem.* **40**, 215 (1978).

[15] C.F. Wu, X. Meng, J. Li, Y.H. Wang, *Acta Phys. Sin.* **58**, 6518 (2009).